Study for CP-violation in the $J/\psi \longrightarrow \Lambda\bar{\Lambda}$ decay

Vincent Hirschi

July 18, 2007

Masters Thesis in High Energy Physics

Directed by:

Prof. Yuanning Gao, Tsinghua University
Prof. Aurélio Bay, Ecole Polytechnique Fédérale de Lausanne

Contents

List of Figures

1 Introduction

This paper studies a possible violation of the charge-parity (CP) symmetry in the $J/\psi \longrightarrow \Lambda\bar{\Lambda}$ decay. The CP-violation has first been observed in the the neutral kaon decays in 1964. However, since then, it has only been seen in very rare decays, as in neutral B decays, and it is still not well-understood. Therefore it is important to find more places where this symmetry is violated to understand what are the underlying principles governing CP-violation and how to best describe it theoretically.

This is done by analyzing a CP-odd observable constructed by the momentum of the decay products of the J/ψ. This work will begin with a short theoretical explanation of the CP-violation, including the appearance of the Cabibbo-Kobayashi-Maskawa (CKM) matrix, the possible CP-violation in the strong interaction and the construction of the observable that will be used. After that, a description of the accelerator and the detector used to record the data is given. The main analysis will focus on how to select the particles to get the best efficiency, before ending with the results obtained with the present data. A short section will also present what can be expected from the data that will be obtained with the future BES III detector.

2 Background Theory

The purpose of this section is to show how to construct an observable based on cinematic quantities which is CP-odd and related to the electric dipole momentum (EDM) of the J/ψ. But before doing this, a short overview of CP-violation and its main mechanism is given.

2.1 A general overview

The first evidence for CP-violation was found in the system of neutral kaons decay. Since then a number of other decays have been found that also violate this symmetry. However the mechanism still remains unclear. Moreover, every violation observed until now has been process-governed by the weak interaction, where CP-violation arises as a second order process in the so-called "box diagram" shown in Figure 1.

These diagrams always contain two charged currents and changes in the flavor of quarks, thus implying a flavor-mixing. This can be described like a rotation in flavor-space where the rotation matrix is known as the CKM matrix. Its parameters can be reduced by gauge transformation to one phase and three angles. Past experiments have attempted to measure these angles to give a better description of this CP-violation.

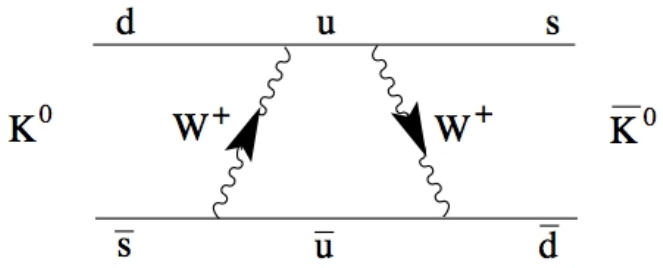

Figure 1: Example of the box diagram for the neutral kaon's oscillation, involving two W's and changing the quark's flavor

The CKM matrix appears in the theory when one adds dynamics to the Lagrangian of the electromagnetic and weak interaction. This is done by transforming the common derivatives into covariant derivatives that cause a CP symmetry breaking in SU(2)×U(1). The simplest lagrangian possible for the Higgs field is:

$$\mathcal{L}_{Higgs} =\mid D_\mu\phi \mid^2 +\mu^2\phi^\dagger\phi - \lambda(\phi^\dagger\phi)^2$$

where μ^2 and λ are real. The coupling of the gauge fields and the quarks is contained in the covariant derivatives, giving each quark the same coupling. Therefore, quark-mixing is not permitted.

However, the Higgs field is not constrained by these considerations because it does not follow from gauge principles. Therefore it allows mixing of quarks as long as one does not impose additional symmetries. Because there are three doublets of quarks, the quarks' fields are written like this :

$$Q_L^i = \begin{pmatrix} u_L^i \\ d_L^i \end{pmatrix} \qquad \text{where} \qquad \begin{array}{rcl} u_L^i & = & (u_L,\, c_L,\, t_L) \\ d_L^i & = & (d_L,\, s_L,\, b_L) \end{array}$$

For right-handed quarks, they are written:

$$u_R^i = (u_R,\, c_R,\, t_R) \qquad \text{and} \qquad d_R^i = (d_R,\, s_R,\, b_R)$$

With this notation, the lagrangian of the interaction between quarks and the Higgs field is written :

$$\mathcal{L} = -\lambda_d^{ij}\bar{Q}_L^i\phi d_R^j - \lambda_u^{ij}\epsilon^{ab}\bar{Q}_{L,a}^i\phi_b^\dagger u_R^j + \text{h.c}$$

where λ_d^{ij} and λ_u^{ij} are general complex coupling matrices. CP would be a symmetry of the system if these matrices were real-valued.

However, by using unitary matrices to redefine the couplings, we can transform these matrices. This corresponds to a rotation in flavor-space. One define U_u and W_u by

$$\lambda_u \lambda_u^\dagger = U_u D_u^2 U_u^\dagger \qquad \lambda_u^\dagger \lambda_u = W_u D_u^2 W_u^\dagger$$

where D_u^2 is the diagonal matrix with positive eigenvalues that gives masses to the quarks. In a similar way, one can define matrices U_d, W_d and D_d.

After that, one can perform the following change of variables.

$$u_R^i \longrightarrow W_u^{ij} u_R^j \qquad d_R^i \longrightarrow W_d^{ij} d_R^j$$

After some calculation, one see that the coupling matrix can be diagonalized, and that the unitary matrices used to perform that disappear from the theory everywhere except in the current that couples the W boson field.

$$J^{\mu +} = \frac{1}{\sqrt{2}} \bar{u}_L^i \gamma^\mu d_L^i \quad \longrightarrow \quad \frac{1}{\sqrt{2}} \bar{u}_L^i \gamma^\mu (U_u^\dagger U_d) d_L^j$$

This $U_u^\dagger U_d$ matrix is known as the CKM matrix [1].

This discussion supposes the simplest Higgs field, namely a single scalar field. However there is no argument that makes this assumption more probable than other assumptions. If we take into account more complex Higgs fields, other couplings can arise, violating CP maximally. Therefore, the exact mechanism that allows CP-violation is still not well-understood, even on theoretical grounds.

2.1.1 Strong CP problem

As mentioned before, one makes a chiral change of variable in the functional integral to give the Lagrangian its final form. The term created here does not have any observable influence because it is a total derivative and therefore disappears when integrating over the whole space. Nevertheless, the term that contains QCD field strength leads to the appearance of an electric dipole moment (EDM) for the neutron, written d_n, which is T-violating.

Experiments have been performed that have imposed a very strong constraint on d_n. It is unclear why this EDM is so close to zero for the neutron. This is known as the *strong CP problem* and has not yet been addressed in any satisfying way. Consequently, the field theory actually predicts a maximal CP-violation in the strong interaction, which has not yet been observed.

There is several possible ways to get a theory that explains why the strong interaction does not violate the CP symmetry. The most famous

[1] For a complete description of the process including more computations, see [6] chapter 20.3

one is a solution involving a new particle called "axion". This solution proposed by Peccei and Quinn considers the violating CP parameter in the QCD Lagrangian to be a field and not a constant. Postulating a new global symmetry to the standard model that will spontaneously be broken, one creates a new Goldstone boson, the axion. However, there is, until now, no evidence of its existence, although several experiments have searched for it. For a more complete introduction on this solution and on the strong CP problem, see [8]. The link with the neutron EDM is detailed in [9].

The very precise measurement of the neutron EDM also gives some upper limit for other particles, using an approximation on the quark structure. However, this limit is generally a loose one and can easily be improved by measurements. This work will investigate more about the EDM of the Λ (which is usually written d_Λ). Some direct measurement has been obtained, but the approach presented here is based on an indirect one, as explained below.

2.2 Studied decay

The decay studied here is $J/\psi \longrightarrow \Lambda\bar{\Lambda}$ where $\Lambda \longrightarrow p\pi^-$ and $\bar{\Lambda} \longrightarrow \bar{p}\pi^+$. It is interesting because very little research has been done on it. The goal is to construct a CP-odd observable with cinematic quantities and then to compute its expectation value. The studied observable is also related to the d_Λ, so that it will bring a new constraint on it.

2.2.1 Basis

The most general amplitude for this decay, were the Λ and $\bar{\Lambda}$ have impulse p_1 and p_2 respectively, can be written like this :

$$A(\ J/\psi\ \longrightarrow \Lambda\bar{\Lambda}) = \\ \epsilon^\mu \bar{u}_\Lambda(p_1) \cdot \Big(\gamma_\mu(a + b\gamma_5) + (p_{1,\mu} - p_{2,\mu})(c + id\gamma_5)\Big) \cdot v_{\bar{\Lambda}}(p_2)$$

In this equation, $\epsilon^\mu = (0, \epsilon)$ is the polarization of J/ψ in its rest frame and a, b, c and d are complex number. CP-violation is equivalent to a non-zero d value.

Knowing the form of the density matrices for $e^+\ e^- \longrightarrow J/\psi$, named here ρ_{ij}, the one for the decay of the J/ψ into two Λ particles (called R_{ij}) and the one for the decay of polarized Λ and $\bar{\Lambda}$, one can give a theoretical expectation value for an observable. The $\Lambda(\mathbf{s_1})$ will decay in $p(\mathbf{q_1}) + \pi^-$, where $\mathbf{s_1}$ is the polarization vector and $\mathbf{q_1}$ the three-momentum of the proton. The decay of $\bar{\Lambda}$ is described by the vectors $\mathbf{s_2}$ and $\mathbf{q_2}$ (and the production of a π^+ instead of π^-). For these decays, the density matrices can be written as :

$$\rho_\Lambda = 1 + \alpha_- \ \mathbf{s_1} \cdot \hat{\mathbf{q}}_\mathbf{1}$$

$$\rho_{\bar{\Lambda}} = 1 - \alpha_+ \, \mathbf{s_2} \cdot \hat{\mathbf{q}}_\mathbf{2}$$

where $\alpha_- \approx \alpha_+ = 0.642 \pm 0.013$.

2.2.2 Observable and expectation value

Using these matrices, the expectation value of any observable is given by:

$$\langle \mathcal{O} \rangle = \frac{1}{N} \int \mathrm{d}\Gamma \; \mathcal{O} \cdot \rho_{ij} R_{ij} \tag{1}$$

Here $d\Gamma$ is the phase space factor of the final state and R_{ij} is the density matrix for the decay of $J/\psi \longrightarrow \Lambda\bar{\Lambda}$ if the two Λ are polarized, a condition to study CP-violation in the system. The factor N gives the normalization given by the equation :

$$N = \int d\Gamma \; \rho_{ij} R_{ij}$$

Since it is impossible to determine directly the polarization of Λ and $\bar{\Lambda}$, one must build an observable based on cinematic data from the product of the decay, implicitly containing it. It is possible to construct many different CP-odd observables but this work only focus on the following two :

$$\mathcal{O}_1 = \theta\big(\hat{\mathbf{p}} \cdot (\hat{\mathbf{q}}_\mathbf{1} \times \hat{\mathbf{q}}_\mathbf{2})\big) - \theta\big(- \hat{\mathbf{p}} \cdot (\hat{\mathbf{q}}_\mathbf{1} \times \hat{\mathbf{q}}_\mathbf{2})\big) \tag{2}$$

$$\mathcal{O}_2 = \hat{\mathbf{p}} \cdot (\hat{\mathbf{q}}_\mathbf{1} \times \hat{\mathbf{q}}_\mathbf{2}) \tag{3}$$

Here $\hat{\mathbf{p}}$ is the unit three-momentum of the Λ, $\hat{\mathbf{q}}_\mathbf{1}$ is the unit three-momentum of the proton and $\hat{\mathbf{q}}_\mathbf{2}$ the one of the anti-proton. $\theta(x)$ is known as the Heaviside step-function and is equal to 1 if $x > 0$ and $\theta(x) = 0$ if $x < 0$. It will clearly change sign if one exchanges the particles with the anti-particles, so that the expectation value has to be zero if CP is conserved. These two observables are almost identical, the only difference being that the second one can take any values while the first one only counts the difference of events that has a positive or negative value. For the sake of simplicity, the expectation value will be computed with $\mathcal{O}_1$ while the figures of the sections 4.6 will represent the value of $\mathcal{O}_2$. The expectation values of the two observables are related by the formula given in the Equation (5).

On the other hand, using the density matrices, it is possible to compute analytically this value. Defining $\beta^2 = 1 - 4m^2/M^2$ where M is the J/ψ mass and m the Λ mass, it gives[2] :

$$\langle \mathcal{O}_1 \rangle = -\frac{\alpha_-^2 \cdot \beta^2}{48N} M^2 \Big(2m \, \mathrm{Re}(da^*) + (M^2 - 4m^2) \mathrm{Re}(dc^*) \Big) \tag{4}$$

[2] see [4]

$$\langle \mathcal{O}_2 \rangle = -\frac{48}{27\pi} \langle \mathcal{O}_1 \rangle \tag{5}$$

We can also see here that $\langle \mathcal{O} \rangle$ will vanish if $d = 0$.

It is also obvious from the form of $\mathcal{O}_1$ that it is equal to

$$\langle \mathcal{O}_1 \rangle = \frac{N^+ - N^-}{N^+ + N^-} \tag{6}$$

where N^+ (N^-) is the number of positive (negative) values recorded for the observable.

To close this section, it is interesting to mention that this observable is independent to the polarization of the J/ψ, to the physical properties of the beam that are contained in the ρ_{ij} matrix, and to the decay of the Λ particles. It only measures CP-violation that could occur in the $J/\psi \longrightarrow \Lambda\bar{\Lambda}$ decay.

2.2.3 Link to d_Λ

It is presently unclear what contributes to the CP-violating term, if there is any. However, it is possible to compute the contribution from different sources, including the electric dipole momentum of the Λ, as presented in [4]:

$$\mathcal{L}_{dipole} = \frac{i}{2} \mathrm{d}_\Lambda \bar{\Lambda} \sigma_{\mu\nu} \gamma_5 \Lambda F^{\mu\nu}$$

The CP-violating interaction, done by the exchange of a photon between Λ and a c quark, is given by the following term:

$$\mathcal{L}_{c-\Lambda} = -\frac{2e\,\mathrm{d}_\Lambda}{3M^2} \cdot \left(p_1^\mu - p_2^\mu\right) \cdot \bar{c}\gamma_\mu \bar{\Lambda} i\gamma_5 \Lambda \tag{7}$$

Combining this last equation with Equation (4) and using the parametrization $< 0 \mid \bar{c}\gamma_\mu c \mid J/\psi >= \epsilon_\mu g_V$, with $\mid g_V \mid$ determined to be 1.25 GeV^2, one gets:

$$d = -\frac{2\,g_V}{3\,M^2}\, e\mathrm{d}_\Lambda \tag{8}$$

In this way, one can relate the expectation value of the observable with d_Λ, using the Equation (4).

The parameter a, b and c can be measured experimentally. However, this have not been measured with enough precision until now. It is assumed that the b factor is much smaller than the two others because it is P-violating while a and c conserves parity. To be able to give an estimation of $\langle \mathcal{O}_1 \rangle$, one has to neglect the b-term. The ones given below assume for the first value that the a-term dominate the computation and the second value assumes it is the c-term that do so.

Here is the computed estimation of $\langle \mathcal{O}_1 \rangle$:

$$|\langle \mathcal{O}_1 \rangle| = \begin{cases} 5.6 \cdot 10^{-3} \frac{\mathrm{d}_\Lambda}{10^{-16} e \text{ cm}} & \text{, in the first case} \\ 1.25 \cdot 10^{-2} \frac{\mathrm{d}_\Lambda}{10^{-16} e \text{ cm}} & \text{, in the second case} \end{cases} \tag{9}$$

From other experiments on Λ, d_Λ is known to be smaller than $1.5 \cdot 10^{-16}$ e cm. Given the theoretical expected value showed in Equation (9), if d_Λ is close to its upper limit, CP-violation may be measurable.

3 Short Overview of BEPC

This research has been performed with data collected with the *Beijing Spectrometer* (BES) detector located in the *Beijing Electron Positron Collider* (BEPC). The following short description will highlight the main points, giving a basic explanation about how each parts work and what is its resolution. More informations can be found in [1].

3.1 Accelerator

The BEPC accelerator is a 202-meters-long linear accelerator ending in a storage ring with circumference of 240 meters. With its beam-energy varying from 2 to 4.2 GeV, it is at this time the only accelerator that is specialized in $\tau -$ charm physics. It is an $e^+ e^-$ symmetric accelerator. The collider is composed of two rings, one for the electron and one for the positron. Its maximum luminosity, for an energy of 1.45 GeV, is equal to $5 \cdot 10^{30}$ cm^{-2} s^{-1}. A sketch is given in the next figure.

It is now upgraded and designed to run with a new detector. The principal improvement is that the time between two bunches is reduced to 8 ns. This will enhance the maximum luminosity of the new accelerator BEPC II up to 10^{33} cm^{-2} s^{-1} (at 1.89 GeV), about two order of magnitude higher than its predecessor.

The best known discovery of BEPC is probably the measure of the τ-mass, the heaviest lepton. It is still the most precise measurement until now, but it will be enhanced with the new data. Since BEPC has permitted very precise measurements on some of the branching ratio of the J/ψ and the Ψ(2s), two charmonium particles, it is expected that the new detector will provide more precise values. Beside that, it is hoped that the very large amount of available data will allow to discover indices of some new physics, either in the mixing of D meson or in the discovery of possible glueballs in the decay of charmed mesons.

Figure 2: BEPC layout

3.2 BES II detector

At the interaction point of the BEPC is located the BES II detector which is illustrated in Figure 3. It is 11 meters long, 6 meters wide and 6.5 meters high.

3.2.1 Vertex chamber - VC

This is the first part of the BES detector. It is a set of 640 straws of 8mm diameter each arranged in 12 layers. Each straw is made of a mylar cylinder with a central 50 μm tungsten wire strung inside. A potential of 3.7 kV is set between the wire and the cylinder, creating a high radial electric field. The straws from layers 1 to 4 and 9 to 12 are axially-oriented while the middle layers make a 3° angle with the beam direction. The layers in the center have to be inclined to reconstruct the track with the greatest accuracy.

This chamber uses the electron produced by the ionized gas produced when a particle crosses a tube. Because of the strong potential near the anode, a shower is induced. Its shape and intensity gives information to the initial ionized molecules, giving the trajectory of the particle. Combining these different pieces of information, the vertex is reconstructed with a resolution of 90 μm.

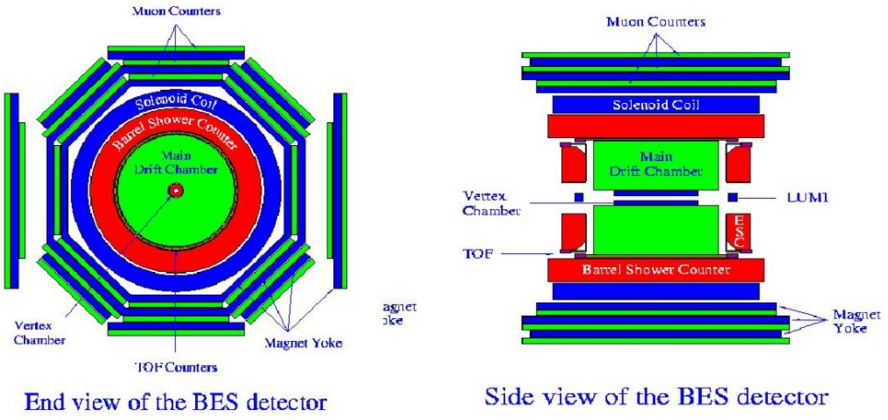

Figure 3: BES detector and its different parts

3.2.2 Main drift chamber - MDC

This part also gives important information to determine the trajectories of particles and to measure the energy loss of charged particles. The chamber contains 804 drift cells and 22936 wires, of which 3216 are sense wire. The other ones are used to shape the electric field into the needed form.

As the studied decay ends up in four charged particles, the information from this part of the detector will have major importance. The curvature of the tracks gives the charge and information on the impulse of particles. To reconstruct the trajectory, the drift chamber uses a principle analogous to the one used in the straw chamber. However, what is used here to capture the signal are the ionized molecules that drift at their limit velocity toward the sense wires. Knowing the time required to reach the sense wire, it is possible to compute precisely where the molecule has been ionized, thus giving a set of points used to fit the trajectory.

The resolution of this part of BES is about 8% for the measure of the $\frac{dE}{dx}$, between 200 and 250 μm for σ_{xy} and about $(1+P^2)^2 \cdot 1.78\%$ for $\frac{\Delta P}{P}$ [3].

The resolution in the new BES III detector will be improved up to 130 μm for σ_{xy}, 0.5% for $\frac{\Delta P}{P}$ and to 6 or 7% for the $\frac{dE}{dx}$.

3.2.3 Time of flight - TOF

The time of flight is measured with 48 scintillator bars covering the whole cylinder. One bar is 284 cm long, 15.6 cm wide and 5 cm thick. This part is used to measure the precise time a particle needs to pass through

[3] Where P is given in GeV

the detector, giving information on its momentum. The resolution is better than 180 ps.

This time will be lower to 90 ps in BES III for the axial part and the end-cap will work with a 110 ps resolution.

3.2.4 Gas barrel shower counter

This part measures the energy of photons and electrons. It is made of 24 layers of gas tubes separated with 23 layers of lead absorber. Each layer contains 560 tubes. Its precision for the $\frac{\Delta E}{E}$ is about 21% and σ_z is around 3 cm.

This is the part that will be enhanced the most in the new detector. σ_z will be lower down to 6 mm and the resolution of $\frac{\Delta E}{E}$ will reach 2.5%. This amelioration will be extremely useful to reconstruct the track with a far better accuracy.

3.2.5 Muon chamber - MC

The muon chamber is composed of 3 layers of iron absorber and three layers of proportional chambers. A chamber contains two sub-layers of four gas tubes. It is used to accurately distinguish if a particle is a muon or not.

The muon chamber will be modified for having 9 layers instead of 3.

3.2.6 A weakness

One can see from Figure 3 that there is no detection for particles following a trajectory that makes only a small angle with the beam pipe. The loss of useful data on certain decay can be of major importance, as will be mentionned later.

An attempt was made to solve this problem by adding some end-caps at the two ends of BES, but unfortunately was not succesful. The consequence is that every track that makes an angle with the beam pipe smaller than 37° (53° for the muon chamber) is lost. This means that about 41% of the track are not recorded by the detector while 59% of the muons do not pass through the muon chamber. For decays that involve a lot of products, this can lead to a huge loss of reconstructed event because this factor must be multiplied by every particles.

However this also will be a major improvement for BES III. Indeed, it will uses end-caps, thus covering a solid angle of $4\pi{\cdot}90\%$ for all its parts, against $4\pi{\cdot}60\%$ for the previous detector. This will lead to a much greater number

of reconstructed events containing all the particles produced. Given also a better luminosity, it is expected that the amount of available data will be a hundred times bigger that what has been collected until now.

Other improvements has been lead to the detector, on which is the improvement of the magnet used to curve the trajectories. The magntic field will be set to 1T (0.4T for BES II).

4 Analyses and Results

This part will focus on the analyses of the data. It will begin by describing the decay and explaining how the different particles have been selected. A discussion about the efficiency and how it is possible to maximize it will also be given before turning to the background. After doing this, the results will be given and the errors computed. The section will end with some future perspectives and ideas to improve the results.

4.1 Decay

As it has been said earlier, the decay discussed here is $J/\psi \longrightarrow \Lambda\bar{\Lambda}$. The J/ψ particle is a $c\bar{c}$ meson, which mass is 3.0969 GeV and full width Γ is equal to 91 keV. The daughter particles are two Λ's, an *uds* baryon weighting 1.115 Gev and showing a mean life time τ of $2.63 \cdot 10^{-10}$ seconds. These two particles will then decay in $p^+\,\pi^-$ (or $p^-\,\pi^+$ for the $\bar{\Lambda}$).

The branching ration (BR) of the first decay will here be assumed to be $2.03 \cdot 10^{-3}$, although the Particle Data Group ([10]) gives a smaller value. The reason is that this measure has been taken with the BESII detector using a large amount of data and is therefore a safer value. Moreover it has been confirmed by another recent experiment. The lower values obtained by previous measurements can also be explained by imprecisions in the MC code that was used at that time. The BR for the decay of the Λ is 0.639, giving a total BR for the complete decay of $8.29 \cdot 10^{-4}$.

BES II has recorded a total amount of 58M J/ψ decays. This means that in these data, there should be about 48000 $J/\psi \longrightarrow \Lambda\bar{\Lambda}$ events. Among these, a lot are not reconstructible because one or more of the four tracks have not passed through the detector. The detector only covers 59% of the solid angle. However, as the direction of the particles are related together, the loss-factor is not just 0.41^4. It is hard to know exactly what it will be, but one can try to give a rough estimation. The Λ will be produced back to back. Because the momentum of the protons are mainly determined by their mother particle, it is possible to assume that they have the same direction. The direction of the pions can differs a lot from the one of the Λ, of about 40 degrees. Therefore, one can consider the decay to have the

equivalent efficiency of three independent particles, giving then an efficiency of $0.59^3 = 21.6\%$. This estimation is a lower limit.

Using a MC sample, it has been shown that this total rate is 27.4%, which is a bit higher. However, this is the efficiency without any cut on the bad tracks, it only represents the number of events of which all tracks go through the detector. After that, one must multiply by the efficiency of the detector to get the final reconstruction rate. This will be done when analyzing the data.

Since these decays always involve only two daughter particles, the energy and momentum are entirely determined by the conservation laws. Given the masses of the particles, one can compute that the Λ will have a momentum of 1.07 GeV. Its energy will be half the mass of the J/ψ. Because the protons weights 938 MeV and the pions only 139 MeV, the momentum of Λ will mainly be transfered to the proton. The direction of the two final paricles will remain close to the one of the Λ. If one computes the momentum of the protons in the Λ rest frame and then boost it to return in the laboratory frame, one finds that it will take value between 0.768 and 1.047 GeV while the pions will vary from 25 to 305 MeV, depending in what direction they are emitted in Λ's rest frame. Their energy is then included in 1.2 an 1.4 for the proton, while E_π takes its values from 140 to 335 MeV. The plots representing these values from Monte Carlo data has been shown in page 13. They show a very good accuracy with the theoretical value. The momentum of the real data are reconstructed with a similar precision.

4.2 Selection of events

4.2.1 Particle-detection

The criteria used in our particle-selection have been very simple. Because of the relative low beam-energy, there are just few particles produced, which is really convenient for the selection. In order to get usable data, some basic cuts are applied :

$P_{\mathbf{tr}} > 70$ MeV where P_{tr} is the transverse momentum. This cut is used to remove the tracks cycling in the MDC.

$|cos(\theta) > 0.75|$ where θ is the angle between a track and the beam's direction. This removes the tracks that are not fully contained in the detector.

It was also asked that the detector identifies two particles as pions and the two other as protons.

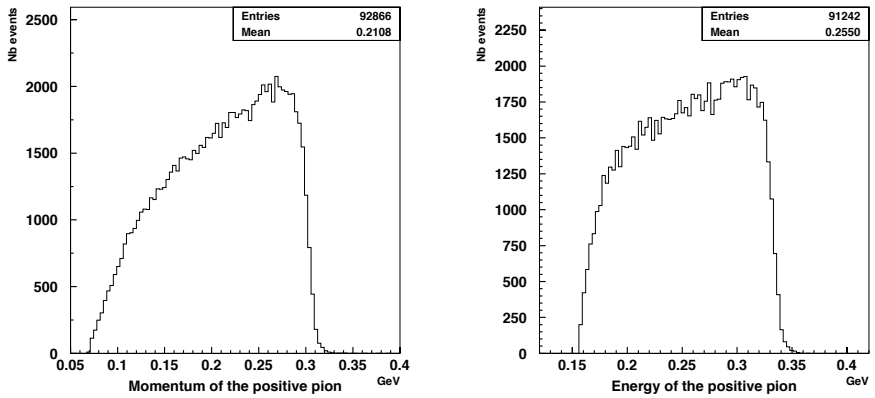

Figure 4: Left: distribution of P_π in the laboratory rest frame for MC data, using only a cut on the mass of the candidate Λ. Right: The same for E_π

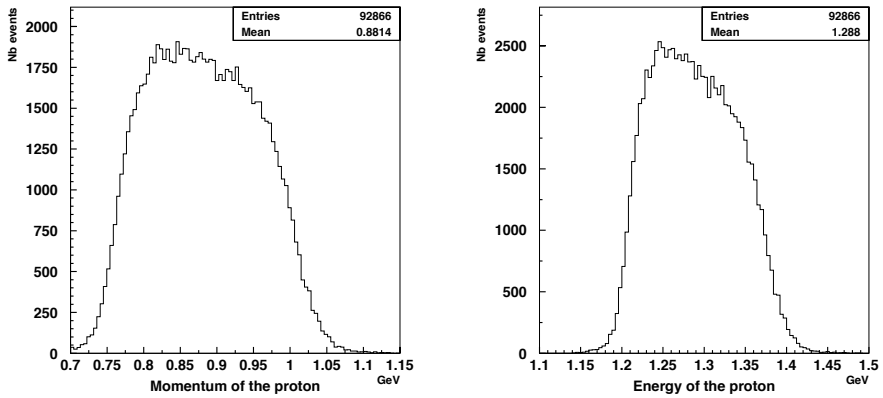

Figure 5: Same thing as the two plots above but this time P_p on the left and E_p on the rignt.

4.2.2 Event-selection

Once the criteria for particle-selection were applied, the very first criterions to select good events has been to get all the decay ending up with exactly four charged tracks. After these basics steps, several additional selection criterions have been applied, giving a window mass for the J/ψ and the two Λ candidates. They are listed below:

- $|M_\Lambda - M_{p^+\pi^-}| < 3\,\sigma = 0.008$ GeV
- $0.98 < p_\Lambda,\, p_{\bar{\Lambda}} < 1.2$ GeV
- $3.02 < E_{J/\psi} < 3.2$ GeV

Here, p_Λ is the momentum of the four-vector given by the sum of the proton and the negative pion and $E_{J/\psi}$ the energy of the four-vector given by the sum of the two Λ.

4.2.3 Testing the channel

The same cuts have been applied in paper [3] and they obtained a sample of 8959 events. In this work, the number of events passing through these cuts has been of 8197. This difference can be explained by the fact that the author used a fit on the two pairs of tracks reconstructing the Λ's to correct the measured impulses. Since the same fit has not been used in this work, the effects of the cuts cannot be identical. However, the fact that the first amount of selected events is near to the second one is a clue that the selection is done properly. Later in this work, another computer code is used to correct the tracks and it leads to a very similar value to the one in cited paper.

4.3 Background and Cuts

In this decay, the background is really low and involves only few other channels. The three main ones are presented below.

4.3.1 $\Sigma^0\bar{\Sigma}^0$

An important source of background is the following decay:

$$J/\psi \quad \longrightarrow \quad \Sigma^0\bar{\Sigma}^0 \quad \longrightarrow \quad \Lambda\gamma\bar{\Lambda}\gamma \quad \longrightarrow \quad p^+\pi^-\gamma\, p^-\pi^+\gamma$$

The BR of the J/ψ decaying into the $\Sigma^0\bar{\Sigma}^0$ is $1.33 \cdot 10^{-3}$ and the decay of Σ^0 into $\Lambda\gamma$ is about 100%. Therefore the total BR is $5.43 \cdot 10^{-4}$. Since Σ has a weight of 1.189 GeV, it is not too far from the Λ and it is possible to confound them when the photon is a soft one.

4.3.2 $\Xi^0\bar{\Xi}^0$

Another possible background would be the decay into two Ξ^0 baryons. The Ξ^0 baryon shows a BR of 99.5% into $\Lambda\,\pi^0$ and its mass is 1314 MeV. Because of its relative high weight with respect of the Λ, the probability to include that sort of events in the selection is fairly weak. It has been tested with a MC sample data five times bigger than the expected statistic and the result was that not a single one event passes the selection-cuts on the mass of the candidate Λ (or candidate $\bar{\Lambda}$). This means that the contamination is virtually inexistent.

4.3.3 $p\bar{p}\,\pi^+\pi^-$

Although this channel is non-resonant, it cannot be neglected because of its large BR. As the particles are not produced in pairs, the chance of reconstructing a candidate Λ passing the cuts is tiny, but since the BR is $6 \cdot 10^{-3}$, which is 10 time bigger than the one of the signal, there is still several events that pass the cuts. As one can see on Figure 6 for the mass of the Λ's, it leads to a continuum.

For these reasons, the only backgrounds that have to be handled are $\Sigma^0\bar{\Sigma}^0$ and $p\bar{p}\,\pi^+\pi^-$. As given above, the BR for the first decay is a little bit lower than the one of the signal. It will now be explored in more details how (or if) it is possible to eliminate these backgrounds in the most efficient way.

The $\Sigma^0\bar{\Sigma}^0$ and the $p\bar{p}\,\pi^+\pi^-$ channels can be seen on Figure 6 representing the mass of the candidate Λ and candidate J/ψ without any other cut than those done for the particle-selection. The first channel can be seen in the bump below the peak at the real mass of J/ψ. It comes from the bad-reconstruced mass of it, because two photons are missing. The second channel is the continuum that one can see on a very large scale over the real Λ mass. The shaded area on the second figure represents the reconstructed mass of the J/ψ candidate for the events that reconstruct it with a momentum lower than 0.2 MeV.

Given the situation of the detector and its low energy, the problems one face are not of the same nature than in the very high energy-range detector, like those in LHC. The goal is not here to separate some tiny signal among a huge amount of backgrounds. The challenge here is to maximize the efficiency of detection in order to get the most meaningful result possible. As it will be shown later, the background is not the major issue, but it is much more a question of finding ways to get more events.

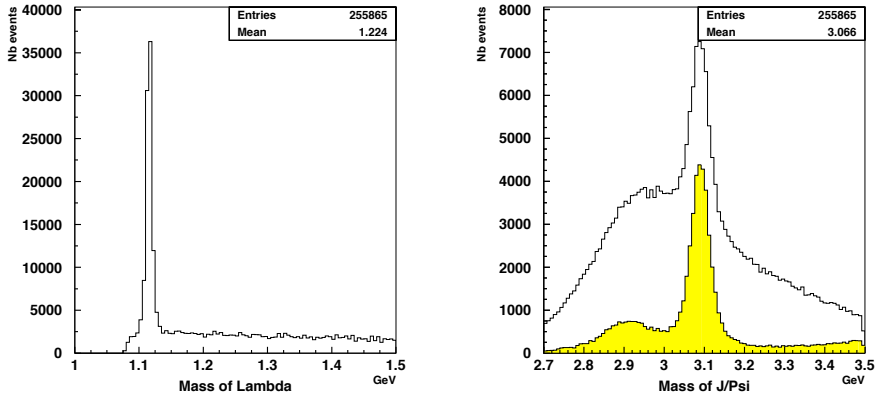

Figure 6: Left: Mass of the candidate Λ. Right: Mass of the candidate J/ψ. The shaded area represents the J/ψ candidate with a momentum lower than 0.2 MeV.

4.4 Treatment of data

Before turning to the suppression of the background, it is useful to come back on the signal and discuss how it is possible to improve it. This will also give an insight to a possible solution for dealing with the $\Sigma\bar{\Sigma}$ events.

4.4.1 KFIT4C

As it has been explained in section 3.2 concerning the detector, the precision is not always very high. A way to try to avoid this imprecision is to fit the observed tracks in new ones that have to obey some constraints. The first one is that the primary vertex remain consistent with the beam size. Then, by giving the candidate protons and pions tracks the exact mass of these particles, one rescales these tracks using the measured energy and direction of the particles, demanding that the total momentum vanishes and that the J/ψ candidate has the exact mass of it.

The program only fit the tracks on one single vertex, thus ignoring the fact that the particles are produces by pairs in two secondary vertex separated by several centimeters. Nevertheless, this does not lead to big errors. The reason is that the major part of the momentum of all final particles are already contained in the two Λ so that the two daughter particles have a similar direction. Correcting the tracks, the fit will have to compensate the particles by pairs to achieve a vanishing total momentum.

A big advantage of this method is that it gives values which are more precise for the momentum and the energy of the two Λ candidate particles. This is shown in Figure 7 where the shaded area represents Monte Carlo data measured without any correction while the peak is the result after this constraint fit. From these figures, it is quite clear that the signal has been

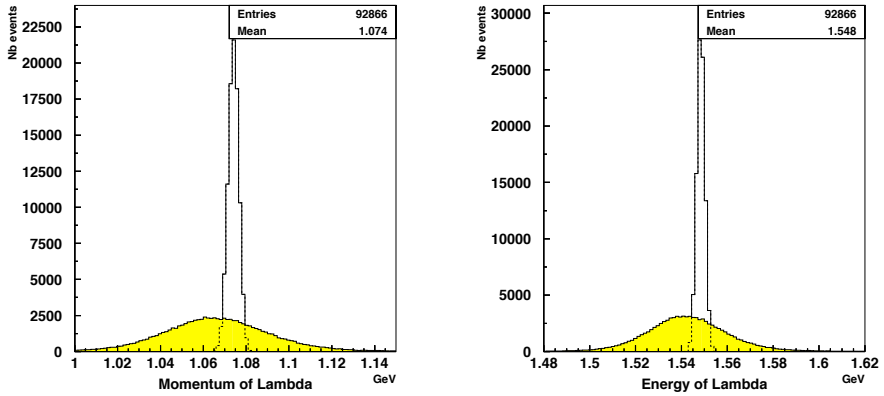

Figure 7: The Momentum (on the left) and the Energy (on the right) of Λ for the tracks before and after the constraint fit for the Λ canditate.

improved.

Another advantage of using this fit, is that it is possible to know how good this fit was, in other words how much it was needed to transform the measured tracks. This information is contained in a χ^2 value. If the fit is absolutely perfect and there is no need to change the tracks, this value vanishes while it gradually increase until it reach 50, a value over which the fit is considered to be of too low accuracy to be useful.

This value is showed in Figure 8 to give an insight of how it is distributed for the signal. A similar figure for the noise will be given later.

Since the background of the Σ^0 channel includes two non-measured photons, the momenta will have to be increased to reach the correct mass for the J/ψ. This effect is showed in Figure 10. Doing this will obligatory lead to a bad fit, leading to a high value of χ^2.

Now that the characteristics of the decays have been explained and that an idea of the tool used to enhance the quality of tracks is given, one can move towards the results and explain the different ways to maximize it.

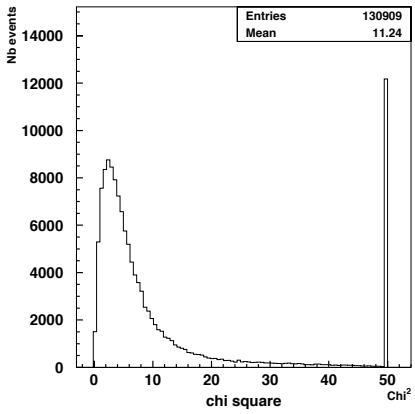

Figure 8: The distribution of the χ^2 value for the signal.

4.5 A battle for efficiency

The goal of the selection and the cuts is to maximize the accuracy of the results. In order to do that, one has to get as much data as possible, while reducing the background. To find the best ratio between these two, one introduce the concept of significance. Several definitions are possible, depending on what are the distribution of the signal and on the background. The two main definitions used are given in Equation (10). They both are usable when the signal and the background present a normal distribution. The first one takes into account the fluctuation of $S + B$ when it is normal distributed. The second one only takes into account the fluctuation of the background, but not of the signal. Here, the signal is referred to as S, the background as B and the significance as $\mathcal{S}$.

$$\mathcal{S}_1 = \frac{S}{\sqrt{S+B}} \qquad \mathcal{S}_2 = \frac{S}{\sqrt{B}} \tag{10}$$

The higher the significance is, the more reliable are the results. Therefore, one as to compute this value for the different cuts.

The analysis with Monte Carlo data will be presented first, and compared to the recorded data at the very end.

4.5.1 Impact on the significance

All the cuts presented here reduce the noise in a good way, but the background is very low from the beginning and the improvement on the significance is only very small. In Equation (10), one has presented two

different possible definitions of the significance. According to $\mathcal{S}_2$, the best one can do in this precise case is to reduce the noise to the minimum, even if one loose some signal doing so. However, according to $\mathcal{S}_1$, given the fact that the noise is a so small proportion, the best way to improve it is to add signal.

4.5.2 A byroad to improve the efficiency

This can be achieved by using a different selection process. Because the accelerator only provides one collision per event, all the detected particles come from the same mother particle. As the background channels are really low, it is possible to use a detection of particles that is not based on the particle identification, but only on their momenta. This has been done by asking for four charged tracks filling the following requirements.

1. Positive charged particle with $P > 0.65$
2. Negative charged particle with $P > 0.65$
3. Positive charged particle with $P < 0.4$
4. Negative charged particle with $P < 0.4$

The efficiency for $\Lambda\bar{\Lambda}$ events after these particle selection-cuts is 27.4% while it was only 23.1% for the ones using particle identification. Of course, this will also lead to an increase of the background, but at the end the significance will rise.

4.5.3 Cuts for $\Sigma^0\bar{\Sigma}^0$

The first background-channel to be handled involves two Σ^0 and two lost photons, therefore will be widely suppressed by the use of KFIT4C. The momentum has to be strongly corrected in most cases because of the energy loss of the photons, therefore a lot of events have a χ^2 equal to 50. Having a look on the χ^2 distribution for $\Sigma^0\bar{\Sigma}^0$, one can see that it increases continuously from very low value up to 50. The $\Lambda\bar{\Lambda}$ events having a completely different form, a cut at 20 will not take off a lot of signal while suppressing the noise up to 84%. Among the 120 events that have a value inferior to 50, only 19 have a value smaller than 20.

Another possibility of cutting off this channel is to use the reconstructed energy for the Λ candidates before correcting it with KFIT4C. Because the photons are not measured, there is a lack of energy for the Λ that clearly appears on the three-momentum norm or on the total energy.

After the correction made by the constraint fit, this effect is no more visible. This shift on the energy is not directly correlated with a bad value

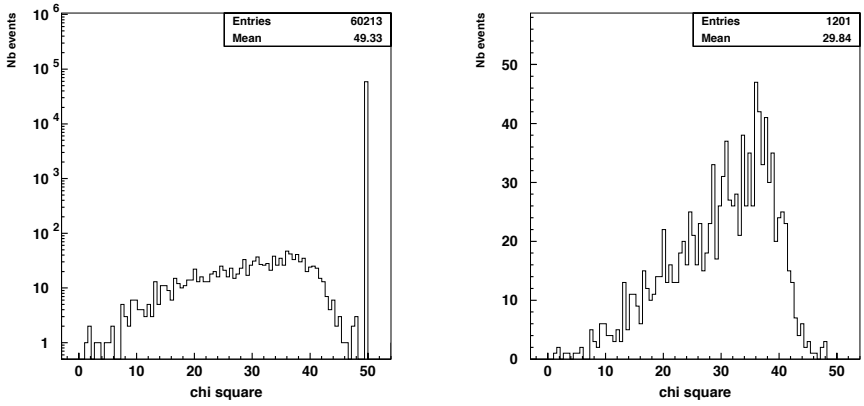

Figure 9: The χ^2 for the $\Sigma\bar{\Sigma}$ channel. The y-scale on the left graphic is given in logarithm in order to see the value below 50.

of χ^2, which means that a cut on too small energies will also remove some of the tracks that have a χ^2 value smaller than 50. To show this, the total energy of the Λ four-vector is represented in the next figure.

As it was showed on Figure 7, the energy of this particle in the signal is also modified to give a much narrower peak, but the old values are centered at the same value as the corrected ones, which is not the case for the Σ channel.

Another possibility is to give the mass-window on the J/ψ and the Λ candidates before or after the use of KFIT4C. The difference is that in the first case, the constraint fit only corrects the tracks that have already pass the mass-window. In the second case, it correct all tracks, and may include new background.

Here is a summary of the different cuts one can apply and their efficiency:

1. Only mass-window, before the constraint fit
2. $\chi^2 < 50$ and mass-window before correction
3. $\chi^2 < 50$ and mass-window after correction
4. $\chi^2 < 20$ and mass-window before correction
5. $\chi^2 < 20$ and mass-window after correction

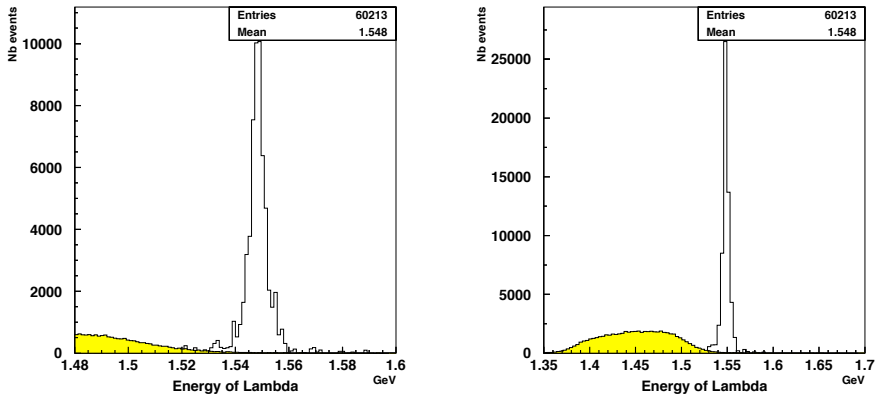

Figure 10: The peak is the energy of the Λ candidate corrected by KFTI4C, the bump standing short before is the non-corrected energy.

	$\Lambda\bar{\Lambda}$			$\Sigma^0\bar{\Sigma}^0$		
Reconstruction	13135			6041		
Cut 1	9334	9334	9285	55	55	46
Cut 2	9287	9273	9197	78	38	19
Cut 3	9124	9124	9077	16	16	12
Cut 4	8886	8877	8812	11	8	5
Cut 5	8802	8802	8756	5	5	4

The second and the third column are the same cuts, but with an additional cut on E_Λ, asking it to be smaller that 1.51 or 1.52 respectively. This table show that if one takes the mass-window on the tracks after KFIT4C, there is no use to add a cut on E_Λ, it would only remove signal. Therefore, this cut will not be used.

4.5.4 Cuts for $p\bar{p}\,\pi^+\pi^-$

For this channel, the situation is not the same: it is a non-resonant background and the constraint fit are here useless. This is because it involves two protons and two pions, without any loss of energy. As KFIT4C is not designed to reconstruct Λ particles, these events will have a very good χ^2.

Because the four particles are entirely independent here, the efficiency is a bit lower of the one of the Λ decay. Among 348000 J/ψ decay in this channel, only 14340 of them are reconstructed.

Since it is a four-body decay, the momentum and energy of the particles are distributed in a continuum. This was visible in the Figure 6. Therefore,

the chance that the four particles all get a momentum that will fit the topology of the decay of two Λ is very low. On a figure of the mass of Λ and $\bar{\Lambda}$, it would be uniformly distributed.

The events that will be include in the mass-window is quite low. It is impossible to remove these remaining events, they have exactly the same properties of the signal. The results of the same cut as defined for the table previous section do not vary very much: they are all equal to 14 except for the two first ones where their is 17 and 16 events that pass the cuts.

4.5.5 Putting the cuts together

Here is given the total result once we put the signal and the two background channels together. There is two different ways to proceed: One can either decide to remove as much background as possible, or keep as much signal a possible. For the first choice, the best is to use a strong cut on χ^2 and use the mass-window on the non-corrected tracks. On the other hand, if one wants to get the largest amount of signal possible, one has two choices. The first one is to release the cut on χ^2 to 50 and then use the mass-window with the corrected tracks. It is also possible to use only the selection done by the mass-window before using the constraint fit, and then correct the tracks once they have been chosen.

Here are the corresponding result:

	Sig	Bckg	$\mathcal{S}_1$	$\mathcal{S}_2$	Data
Cut 1	8802	19	93.7	2024	7989
Cut 2	9287	94	95.9	957	8629
Cut 3	9334	72	96.2	1098	8939

where the cuts are defined by:

1. $\chi^2 < 20$ and old mass-window
2. $\chi^2 < 50$ and new mass-window
3. Only old mass-window

and where the last column represents the real data. These three ways to select the events are almost equivalent, the difference in the significance is only marginal.

One can see that the number of real data is a always a bit lower than what was expected from Monte Carlo. Given the fact that the number of reconstructed events are the same, it means that the efficiency of the cuts for MC data is bigger than for real data. The reason is that the precision of the tracks measured by the detector is a bit lower than what is computed by the simulation, causing more losses after the cuts.

In order to show that the selection is done properly, on can plot the reconstructed mass for the candidate Λ and the one for the candidate $\bar{\Lambda}$. These distributions are shown in Figure 11.

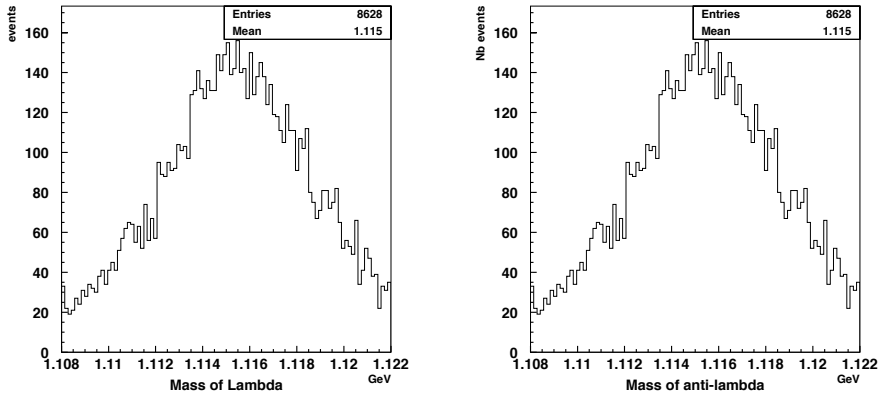

Figure 11: Mass of Λ and $\bar{\Lambda}$.

4.6 Final results and errors

The goal of all these cuts was to get the best signal possible. Now that they have been chosen, they will be applied on real data. The distribution of the observable is given in Figure 12.

The shape of the distribution is not important and has no physical meaning. The formula to compute it was a product a several vectors, so that a lot of terms contributes to the exact value, but in a complicated way. The only physical interesting parameter is here the mean value. Once that it is known, one can also compute the error to find if it is consistent with zero or not. A short explanation on the way the error is computed is given first.

4.6.1 Statistical error

As explained in the theoretical part, the statistical error will be computed using the first observable, $\mathcal{O}_1$ given in Equation (2). This means that the exact value of the observable is meaningless and that only its sign matters. As it can only take two different values, it will obey a binomial law. If there is no CP-violation, the parameter p, defined by the probability to get a positive value, will be equal to 1/2.

To get the mean value of the distribution of the observable, one varies the parameter p and computes which one best describes the measured results. This method is explained in more details in annex A, but as it is just

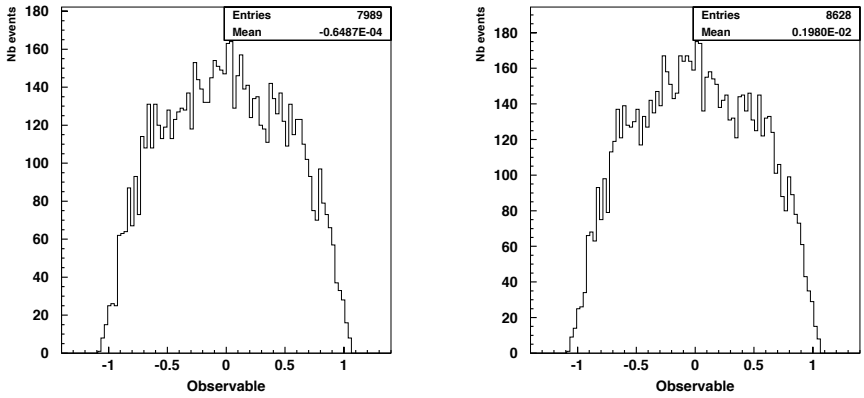

Figure 12: Two distribution of the observable using real data. On the left using the cut 1 and the cut 2 on the right.

mathematical statistics, the computations are of no interest here. Therefore, only the results will be presented.

As one can see from the graphics of the observable, it is equally distributed on positive or negative values. The expectation value for the observable has been computed for the three ways of selecting the particles given above. The result is:

$$\begin{array}{ll} 1 & 1.87 \cdot 10^{-3} \pm 1.73 \cdot 10^{-2} \\ 2 & 3.25 \cdot 10^{-3} \pm 1.55 \cdot 10^{-2} \\ 3 & 6.15 \cdot 10^{-3} \pm 1.15 \cdot 10^{-2} \end{array}$$

On can see that all of them remain consistent with zero, the result we were expecting (altough it would have been very exciting if the result would have been found to be different!). Therefore, as far as one can know, there is no CP-violation in the $J/\psi \longrightarrow \Lambda\bar{\Lambda}$ decay. The mean value for the observable is smaller than $1.75 \cdot 10^{-2}$ with a confidence level of 95%. The data provided in the future BES III detector will enable a improvement of this measurement.

4.6.2 Resulting constraint on d_Λ

One can now try to put a new constraint on the electric dipole momentum for the Λ. Equation (9) give the link between them. The next table gives the d_Λ value computed for the three cuts and its respective error. Recall the actual upper value for d_Λ is $1.5 \cdot 10^{-16}\ e\,\mathrm{cm}$. All the value given here are in the same unit.

	a dominant	c dominant
1.	0.33 ± 3.09	0.15 ± 1.38
2.	0.58 ± 2.77	0.26 ± 1.24
3.	1.09 ± 2.05	0.48 ± 0.92

Therefore, the conclusion is that if the dominant term is a, this experiment gives no new upper limit and the error is too large to give any new information. If the dominant term is c, then the upper limit of d_Λ is $1.4 \cdot 10^{-16}\, e\,\mathrm{cm}$ with a confidence level of 95%, a little bit better than the previous measurement.

4.6.3 Systematic error

A complete discussion on the results should include a discussion on the systematic error. Unfortunately, this was not possible in the scope of this work. Such a study would demand some more MC analysis and comparison between reference tracks and how it is recorded. Moreover, given the form of the observable, the propagation of the error is quite complex and cannot be handled lightly.

It is expected that it is larger than the statistical error, but it is hard to give an approximation for it.

4.7 Future perspectives

As one can see now, this research only confirms what was already known. The precision on the electric dipole moment of the Λ stands in the order of magnitude of what has previously been measured. Concerning the CP-violation, it seems that it does not occur in this decay, as it was expected.

However, this does not mean that no further research should be done on this channel. In the near future, the BES III detector will begin to take new data, and it is expected that it will store up about 100 times more data of J/ψ decay. In addition, because of the improvement of the detector, the precision of the particles' tracks and their energy will be much higher. These more accurate data will lead to a better efficiency when reconstructing the decay. With these two changes put together, it may be possible to enhance the precision on the expected value of the observable by one order of magnitude, maybe by a factor twenty.

Using the electromagnetic calorimeter could also lead to a better event-selection. As the main background is $\Sigma^0\bar{\Sigma}^0 \longrightarrow \Lambda\Lambda\gamma\gamma$, it can be well eliminated by cutting every event that has two hits in it.

4.7.1 Ways to improve the results

Another possible improvement to cut the background coming from the $\Sigma^0\bar{\Sigma}^0$ decay would be to use a second vertex fit on the Λ particles. If they

come directly from the J/ψ, they are emitted in opposite direction. On the contrary, if a Σ^0 stands in between, the photon will change the direction of emission. Because Λ has a $c\tau$ of 7.89 cm while the one of Σ^0 is $2.2 \cdot 10^{-9}$cm, this can be verified. With the vertex fit, it is possible to compute the momentum of the particle that decay in the second vertex. Measuring then the $cos(\theta)$ for this direction, it is possible to make a cut on $cos(\theta_1) + cos(\theta_2)$, the two angles formed by the Λ.

It has been tried in this study and it has been shown that it is indeed a very good way to get rid of this background. It cuts about 70% of this channel for events where the two secondary vertices are well reconstructed. However, with the present data, this cut would eliminate far too much signal. In fact, only one third of the reconstructed events have a good reconstruction of their two secondary vertices. But if the precision achieved with BES III allow it, it could be a good way of getting a really pure signal.

But beside this enhancement of the detection, it is also possible to work further for a better accuracy in the final result. As it has been explained before, the KFIT4C code that was used here does not force the creation of the Λ particles. Within the range of precision of BES II, this was not a handicap. However, using the BES III in its full possibilities, a new code that would include this feature would permit a better fit of the tracks and lead to a powerful tool in the reconstruction of the signal and elimination of the background.

5 Conclusion

It has been shown in this work how it is possible to measure a possible violation of the CP-symmetry in the $J/\psi \longrightarrow \Lambda\bar{\Lambda}$ decay. The underlaying theory has been presented and it has been explained why and how it could occur. The result found was that there is, for the moment, no experimental evidence of a CP-violation. Concerning the value of the Λ's electric dipole momentum, the result are in good coherence with the previous measurement, using direct technics. However, it was not possible to give a better estimation of it.

According to this description, this research could seem that it was not really successful. Nevertheless, it was shown that it is indeed possible to give a value for d_Λ that was very near of the limit of what is already known. But this means that it will be possible to give a more precise measurement using the data collected with the new BES III detector. This new J/ψ factory will produce enough particles in order to enhance this value by one order of magnitude at least. Therefore, the approach presented here remain a good valid one to improve or confirm the characteristics of the Λ.

For the CP-violation part, it is harder to give a clear conclusion. The result shows that there is no violation in this decay as far as one can see. But this was actually what was expected. No CP-violation has been observed in the strong interaction until now, and it would have been quite surprising if it would have occurred here so close for the limits given by indirect constraints. However, here also the limit given in this work can be improved by one order of magnitude using the new data that will be provided by BES III. Since the theory is unable to give a complete description of how this symmetry breaks, it is really important to find other decays where it is the case. Unfortunately, it seems that this channel is not very successful, at least according to the present possible precision. But it is still important to continue to look after it.

Maybe, as often in physics, the experiment that will lead to find a new a completely unexpected violation of CP in some channel will discover it while searching for something else. The fortune sometimes has tricky ways of dealing with progress. Keep searching it, someday it will show up.

A Statistical error

This section is devoted to the computation of the statistical error of the expectation value of the observable. Its form is recalled here :

$$O = \theta\big(\hat{\mathbf{p}} \cdot (\hat{\mathbf{q}}_\mathbf{1} \times \hat{\mathbf{q}}_\mathbf{1})\big) - \theta\big(- \hat{\mathbf{p}} \cdot (\hat{\mathbf{q}}_\mathbf{1} \times \hat{\mathbf{q}}_\mathbf{1})\big)$$

As one can see, it can only take two different values, 1 or -1. Therefore it lead to a binomial distribution. The interesting thing is to know if this distribution shows an equal probability to get both events. If it is the case, it also means that the expectation value of the observable is null.

In the experiment, one measures a certain amount of positive and negative values. The former will be called N^+ and latter N^-. The expectation value can be written in this way :

$$\langle O \rangle = -\frac{N^+ - N^-}{N^+ + N^-}$$

Defining a parameter g to measure the deviation from the $1/2$ probability, it is possible to find the probability of getting N^+ for a given amount of N total events.

$$g := \frac{\mathcal{N}^+}{N^+ + N^-} \qquad \text{and} \qquad \mathrm{P}(N^+, N, g) = \frac{N!}{N^+!\,(N - N^+)!} \cdot g^{N^+} (1-g)^{N-N^+}$$

The number N^+ is measured and $\mathcal{N}^+$ is a variable. The value of g at the maximum of the density probability function P indicates what is, most likely, the probability of getting an event with a positive value for the observable.

Instead of searching for the maximum, one computes the minimum of the function $-\ln(\ \mathrm{P}(N^+, N, g)\ )$. Then, the error on g is simply measured by the difference between the value g_1 and g_2, the two points given by $\mathrm{P}^{-1}(\mathrm{P}(N^+, N, g_{\min}) + 1/2)$.

Acknowledgments

Finally, I want to give special thanks to Professor Gao who has been very kind and available for numerous questions of all kind. I also want to thank his PhD students who helped us in the beginning of our stay in China.

I also thank Professor Bay and the people at EPFL who has made this year in Tsinghua University possible.

References

[1] J.Z. Bai et al.: The BES upgrade, Nuclear Instrumentation and Methods in Physics Research A 458, July 2000.

[2] BES collaboration (M. Ablikim et al.): BES II detector simulation, Nuclear Instrumentation and Methods in Physics Research A 552, July 2005.

[3] BES collaboration, M. Ablikim et al.: Study of the J/ψ decay to $\Lambda\bar{\Lambda}$ and $\Sigma^0\bar{\Sigma}^0$, Physics letters B 632, November 2005

[4] Xiao-Gang He, J.P. Ma and Bruce McKellar CP-violation in $J/\psi \longrightarrow \Lambda\bar{\Lambda}$, Physical Review D, Volume 47 number 5, March 1993.

[5] Xiao-Gang He, J.P. Ma and Bruce McKellar: CP-violation in fermion pair decays of neutral bosons particles, Physical Review D, Volume 49 number 9, May 1994.

[6] M.Perskin, D.V. Schroeder: An Introduction to Quantum field theory, Westview Press, 1995.

[7] M. Maggiore: A modern introduction to Quantum Field Theory, Oxford University Press, 2005.

[8] Michael Dine: Lectures on the strong CP problem, hep-th/0011376, November 2000.

[9] Jiang Liu, C.Q. Geng and John N. Ng: Strong CP Violation and Neutron Electric Dipole Moment Physical Review Letters, Volume 63 number 6, August 1989.

[10] S.Eidelman et al. Particle Physics booklet, Physics Letters B592, 1, 2004.